



**Proceedings of the 7th International Conference on HydroScience and Engineering
Philadelphia, USA September 10-13, 2006 (ICHE 2006)**

ISBN: 0977447405

Drexel University
College of Engineering

Drexel E-Repository and Archive (iDEA)
<http://idea.library.drexel.edu/>

Drexel University Libraries
www.library.drexel.edu

The following item is made available as a courtesy to scholars by the author(s) and Drexel University Library and may contain materials and content, including computer code and tags, artwork, text, graphics, images, and illustrations (Material) which may be protected by copyright law. Unless otherwise noted, the Material is made available for non profit and educational purposes, such as research, teaching and private study. For these limited purposes, you may reproduce (print, download or make copies) the Material without prior permission. All copies must include any copyright notice originally included with the Material. **You must seek permission from the authors or copyright owners for all uses that are not allowed by fair use and other provisions of the U.S. Copyright Law.** The responsibility for making an independent legal assessment and securing any necessary permission rests with persons desiring to reproduce or use the Material.

Please direct questions to archives@drexel.edu

REYNOLDS NUMBER EFFECT ON THE INTERACTION OF AN ELASTIC CIRCULAR CYLINDER AND ITS AMBIENT FLUID FLOW

Shain-Woei Jeng¹ and Chieh-Chih Lu²

ABSTRACT

The vortices shedding from the downstream surface of a cylindrical structure cause periodic variations of the lift and drag forces, which then produce vibrations. The vibration also changes the pattern of vortex shedding. This mutual effect is called fluid-structure interaction. The interaction of a rigid cylinder supported elastically and its ambient incompressible fluid flow was simulated numerically in this study. The flow field is obtained first by solving the Navier-Stokes equations using the primitive method. Then, the lift and drag forces on the cylinder are computed. With the forces, the vibration of the cylinder may be calculated by applying Newton's second law of motion. At the next time step, the motion of the cylinder decides the boundary conditions and the acceleration term of the momentum equation since a moving coordinate system is adopted for the flow field calculation. The objective of this paper is to discuss the Reynolds number (Re) effect on this interactive system. Results showed that the cylinder moved periodically along a figure"8" path. At lower Re, the peak lift force in the resonant region was significantly higher, and the natural frequency at which peak lift occurred was larger. The Re-effect on the resonant region, the root mean square of the lift force, the time average of the drag force, and cylinder vibration are also discussed in this paper.

1. INTRODUCTION

For incompressible fluid flow past an elastic circular cylinder (rigid circular cylinder supported elastically), the vortices shed alternatively from behind the cylinder. This vortex shedding causes periodic lift and drag forces, which produce cylinder vibrations in both longitudinal and transverse directions. Finally the cylinder vibrations affect vortex shedding. This phenomenon is called fluid-structure interaction. When the natural frequency of the cylinder is close to the shedding frequency of the vortices, the amplitude of the vibration increases, and synchronization occurs. The vibration could cause damage to the cylindrical structure and might lead to break down of the structure. This type of numerical simulation was developed in the 1990's and plays an important role in the field of engineering applications.

Related studies may trace back to flow past a fixed circular cylinder [5] [8] [9], to flow past a forced vibrating cylinder both in the transverse direction [1], and in the in-line direction [12] [13],

¹ Professor, Department of Water Resources Engineering, Feng-Chia University, Taichung, Taiwan, R. O. C. (swjeng@fcu.edu.tw)

² Graduate Student, Department of Water Resources Engineering, Feng-Chia University, Taichung, Taiwan, R. O. C. (P9432716@fcu.edu.tw)

and to flow past a forced rotational cylinder [3] [10] [11]. Recently, as the progressing of computer, the numerical study of this issue became more workable. The interaction between flow and the cylinder has been simulated by numerical models [2] [7] [14].

This paper discusses the Reynolds number effect on the interactive system [4], for example, the Reynolds number effect on the band width of the resonant zone, the root mean square of the lift force, the time-averaged value of the drag force, and the vortex shedding. The path of the cylinder vibration is also discussed in this paper.

2. METHODS

2.1 Flow Field

The flow field is solved on a non-inertial moving coordinate, that is not rotating with the cylinder. The non-dimensional incompressible momentum equation can be written as:

$$\frac{\partial \mathbf{V}}{\partial t} = -\nabla P + \mathbf{VS} - \mathbf{CN} - \ddot{\mathbf{Z}} \quad (1)$$

where \mathbf{V} , P , \mathbf{VS} , \mathbf{CN} and $\ddot{\mathbf{Z}}$ are the velocity vector, pressure, the viscous term, the convective term, and the rectilinear acceleration of the cylinder, respectively.

Introducing an intermediate velocity ($\hat{\mathbf{V}}$) and using a time-splitting technique [6], Eq. (1) may be split into two steps:

$$\frac{\hat{\mathbf{V}}^{n+1} - \mathbf{V}^n}{\Delta t} = \mathbf{VS}^{n+1/2} - \mathbf{CN}^{n+1/2} - \ddot{\mathbf{Z}}^{n+1/2} \quad (2)$$

$$\frac{\mathbf{V}^{n+1} - \hat{\mathbf{V}}^{n+1}}{\Delta t} = -\nabla P^{n+1/2} \quad (3)$$

where “n” denotes a time step. It can be shown that these equations have a second order accuracy in the time domain. Applying the continuity equation yields:

$$\nabla \cdot \mathbf{V}^{n+1} = 0 \quad (4)$$

The divergence of Eq. (3) yields:

$$\nabla^2 P^{n+1/2} = \frac{1}{\Delta t} \nabla \cdot \hat{\mathbf{V}}^{n+1} \quad (5)$$

Eq. (2) is solved first for $\hat{\mathbf{V}}^{n+1}$. Then $P^{n+1/2}$ is obtained from Eq. (5). Finally, Eq. (3) is solved for \mathbf{V}^{n+1} to complete a time-step calculation for the flow field. Eq. (5) is solved by employing a SOR (successive over relaxation) scheme.

The (r, θ) plane is transformed into the (ξ, η) plane according to (see Figures 1 and 2)

$$r = \exp(\pi\xi) \quad \theta = \pi\eta \quad (6)$$

By setting $\Delta\xi=\Delta\eta = \text{constant}$, the size of the grids on (r, θ) plane is enlarging in the r direction. A backward staggered grid system is adopted for the calculation.

2.2 Cylinder Vibration

A circular cylinder supported elastically in the flow field is shown in Figure 3. The equation of two-dimensional vibration on an inertial coordinate is

$$\ddot{\mathbf{Z}} + 4\pi\zeta f_n \dot{\mathbf{Z}} + 4\pi^2 f_n^2 \mathbf{Z} = \frac{\mathbf{C}_F}{M} \quad (7)$$

where \mathbf{Z} is the cylinder displacement, $\dot{\mathbf{Z}}$ the cylinder velocity, $\ddot{\mathbf{Z}}$ the cylinder acceleration, \mathbf{C}_F the force vector, M the mass ratio, f_n the natural frequency, and ζ the damping ratio (damping coefficient / critical damping coefficient). $M = \pi \rho_c / 2$, where ρ_c is the density ratio (density of the cylinder / the fluid density).

2.3 Interaction

In each time step of the calculations, the new \mathbf{V} and P of the flow are calculated first based on the variables at the present time step. Then the drag (CD) and lift (CL) forces exerted on the cylinder may be computed. Finally, the vibrations of the cylinder are solved. The interaction between the fluid flow and the elastic cylinder is achieved through the renew of the variables $\ddot{\mathbf{Z}}$, CD and CL, and the resetting of the boundary conditions.

2.4 Tow-Stage Modeling

Modeling is completed in two stages. In the first stage, no vibration is allowed (referred to as the “fixed” case), and the relative uniform-flow velocity is set to be the time-averaged terminal velocity determined by Re. An artificial disturbance, similar to that used by [5], is applied to generate periodic vortex shedding. The non-dimensional time for the first stage is commonly 100. In the second stage, the fixed cylinder is released, and becomes a freely vibrating cylinder. Then the flow field starts interacting with the cylinder.

2.5 Calculated Condition

In most of the cases, $\Delta t=0.01$, $\Delta\xi=\Delta\eta=0.02$, and there are 80×100 grids in r and θ directions respectively. The calculation is proceeded to $t=100 \sim 200$ for the second stage. Details and verification of the model are given in [4].

3. RESULTS AND DISCUSSION

3.1 Some characteristics of the fluid-cylinder system

Based on $Re=100$, $\rho_c = 2$, and $\zeta = 0$, this section discusses some characteristics of the fluid-cylinder system. Results showed that the cylinder center moved periodically along a figure “8” path, as shown in Figure 4. The path started at point A, moved up rightward to B, and finally went back

to point C, which coincided with point A. This completed one-half of the periodic motion. The left side of the path is symmetrical to the right side. The amplitude of the transverse vibration ($XC_{\max}=1.2$) was about twenty times larger than that of the in-line vibration ($YC_{\max}=0.065$).

Figure 5 shows the periodic vibration curves of the forces and the cylinder displacements. XC and YC are the transverse and in-line displacements of the cylinder, CL is the lift coefficient, and $CD' = CD - \overline{CD}$, where CD is the drag coefficient and \overline{CD} is the time-averaged value of CD . Those curves resemble sine functions. The phase lag between the force and the displacement can be obtained from the figure. That the amplitude of the transverse vibration is about twenty times greater than that of the in-line vibration may also be seen from the figure.

3.2 Vibration Zones

In accordance with the vibration characteristics, this study divided the natural frequency of the cylinder into three zones, i.e. synchronization zone (S-zone), non-synchronization zone (NS-zone), and buffer zone (B-zone), which was between S-zone and NS-zone. The details of the divided methods can be found in [4].

The resonant zones at different Re are listed and drawn in Table 1 and Figure 6. As Re increased, the S-zone and the lower NS-zone became smaller. When $Re=80$, there was no low B-zone.

3.3 Effect of Reynolds number

At $\rho_c = 2$ and $\zeta = 0$, this section discusses the Reynolds number (Re) effect on this interactive system. The vortex shedding frequency (f_0), lift force (CL_0), and drag force (CD_0) for fixed-cylinder case at different Re are listed in Table 2.

Figure 7 shows the curve of the lift force ratio (CL_{rms} / CL_0) versus the natural frequency ratio (fn/f_0) at different Reynolds number, where CL_{rms} is root-mean-square of the lift force, CL_0 is root-mean-square of the lift force for fixed-cylinder case, and f_0 is the shedding frequency for fixed-cylinder case. The trends of the curves are very similar. From left to right, these curves forward to a minimum value the increase to a maximum value, after which they drop to a constant equal to 1. As Reynolds number increases, the peak of CL_{rms} / CL_0 decreases, and the corresponding frequency ratio of the peak decreases.

Figure 8 shows the curves of the drag force ratio (CD_{avg} / CD_0) versus the natural frequency ratio (fn/f_0) at different Reynolds number, where CD_{avg} is the time-averaged drag force, and CD_0 is the time-averaged drag force for the fixed-cylinder case. The trends of the curve are very similar to those of CL . As Reynolds number increases, the peak of CD_{avg} / CD_0 mildly increases, and the corresponding frequency ratio of the peak decreases.

4. CONCLUSION

A numerical model was formulated to simulate the interaction between fluid flow and an elastic circular cylinder. The Reynolds number (Re) effect on this interactive system at variant natural frequency of the cylinder was studied.

Results showed that the center of the cylinder moved periodically along a figure "8" path. The amplitude of the transverse vibration was twenty times larger than that of the in-line vibration at a certain test condition. There was phase lag between the force and the cylinder displacement.

According to the vibration characteristics, this study divided the natural frequency of the cylinder into synchronization zone (S-zone), non-synchronization zone (NS-zone), and buffer zone

(B-zone). As Re increased, the S-zone and the low NS-zone became smaller. There was no low B-zone at $Re=80$.

At different Reynolds number, the trends of the curves of the lift force ratio were very similar. As Re increased, the peak of the lift force ratio decreased, the peak of the drag force ratio mildly increased, and the corresponding frequency ratios for both peaks decreased.

REFERENCES

1. Cheng, C. H., J. L. Hong, and W. Aung, 1997, Numerical Prediction of Lock-on Effect on Convective Heat Transfer From a Transversely Oscillating Circular Cylinder, *Int. J. Heat Mass Transfer*, Vol. 40, No. 8, pp. 1825~1834.
2. Evangelinos, C., D. Lucor, and G. E. Karniadakis, 2000, DNS-Derived Force Distribution on Flexible Cylinders Subject to Vortex-Induced Vibration. *J. Fluids and Structures*, Vol. 14, pp. 429~440.
3. Filler, J. R., P. L. Marston, and W. C. Mih, 1991, Response of the Shear Layers Separating from a Circular Cylinder to Small-Amplitude Rotational Oscillations, *J. Fluid Mech.*, Vol. 231, pp. 481~499.
4. Jeng S. W. and C. C. Lu, 2005, Simulation of the Interaction System for a Flow Past an Elastic Circular Cylinder, memoir of Feng-Chia University, pp. 1~97.
5. Jordan, S. K. and J. E. Fromm, 1973, Oscillatory Drag, Lift, and Torque on a Circular Cylinder in a Uniform Flow, *The Physics of Fluids*, 1972, Vol. 15, No. 3, pp. 371~377.
6. Lu, X. Y. and J. Sato, 1996, A Numerical Study of Flow Past a Rotationally Oscillating Circular Cylinder, *J. Fluids and Structures*, Vol. 10, pp. 829~849.
7. Newman, D. J. and G. Karniadakis, 1997, A Direct Numerical Simulation Study of Flow Past a Freely Vibrating Cable. *J. Fluid Mech.*, Vol. 344, pp. 95~136.
8. Oseen, C. W., 1910, Über die Stokesche Formel und über die verwandte Aufgabe in der Hydrodynamik, *Arkiv Mat., Astron., Fysik*, 6(29).
9. So, R. M. C., Y. Liu, and K. Lam, 2001, Numerical Studies of a Freely Vibrating Cylinder in a Cross-Flow, *J. Fluids and Structures*, Vol. 15, pp. 845~866.
10. Taneda, S., 1978, Visual Observation of the Flow Past a Circular Cylinder Performing a Rotary Oscillation, *J. Physics Society of Japan*, Vol. 45, pp. 1038~1043.
11. Tokumaru, P. T. and P. E. Dimotakis, 1991, Rotary Oscillation Control of a Cylinder Wake, *J. Fluid Mech.*, Vol. 224, pp. 77~90.
12. Williamson, C. H. K., 1985, Sinusoidal Flow Relative to Circular Cylinders, *J. Fluid Mech.*, Vol. 155, pp. 141~174.
13. Zhang, J. and C. Dalton, 1993, A Numerical Comparison of Morison Equation Coefficient for Low Keulegan-Carpenter Number Flows : Both Sinusoidal and Nonsinusoidal, *J. Fluids and Structures*, Vol. 7, pp. 39~56.
14. Zhou, C. Y., R. M. C. So and K. Lam, 1999, Vortex-Induced Vibrations of Elastic Circular Cylinders. *J. Fluids and Structures*, Vol. 13, pp. 165~189.

Table 1 The resonant zones at different Reynolds number.

	Re=80	Re=100	Re=200
Low NS-zone	$f_n/f_0 < 0.67 \pm 0.07$	$f_n/f_0 < 0.62 \pm 0.07$	$f_n/f_0 < 0.52 \pm 0.06$
Low B-zone		$0.62 \pm 0.07 < f_n/f_0 < 0.96 \pm 0.05$	$0.52 \pm 0.06 < f_n/f_0 < 0.81 \pm 0.04$
S-zone	$0.67 \pm 0.07 < f_n/f_0 < 1.53 \pm 0.05$	$0.96 \pm 0.05 < f_n/f_0 < 1.51 \pm 0.03$	$0.81 \pm 0.04 < f_n/f_0 < 1.35 \pm 0.02$
High B-zone	$1.53 \pm 0.05 < f_n/f_0 < 1.85 \pm 0.03$	$1.51 \pm 0.03 < f_n/f_0 < 1.93 \pm 0.08$	$1.35 \pm 0.02 < f_n/f_0 < 1.62 \pm 0.06$
High NS-zone	$1.85 \pm 0.03 < f_n/f_0$	$1.93 \pm 0.08 < f_n/f_0$	$1.62 \pm 0.06 < f_n/f_0$

Table 2 The vortex shedding frequency, lift coefficient, and time-averaged drag coefficient for fixed-cylinder case at different Re.

	f_0	CL_0	CD_0
Re=80	0.0747	0.153	1.34
Re=100	0.0804	0.210	1.32
Re=200	0.0955	0.429	1.31

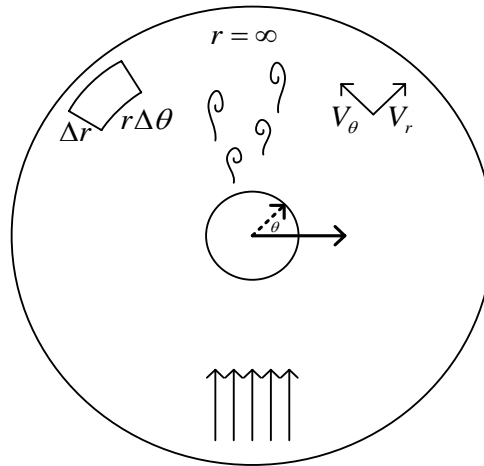


Figure 1 The (r, θ) plane.

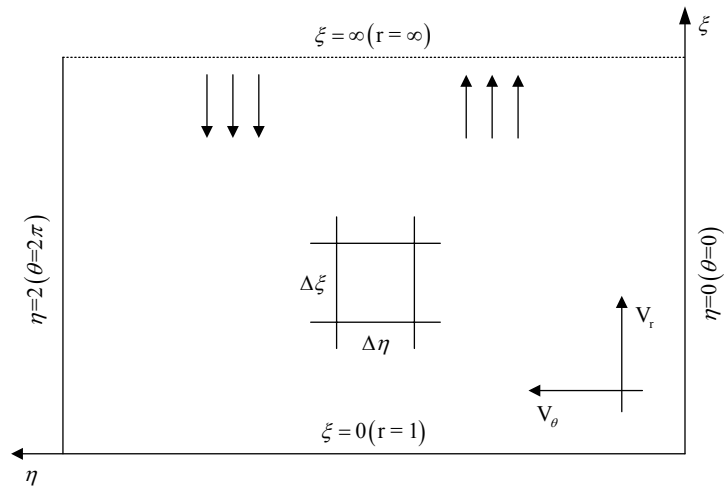


Figure 2 The (ξ, η) plane.

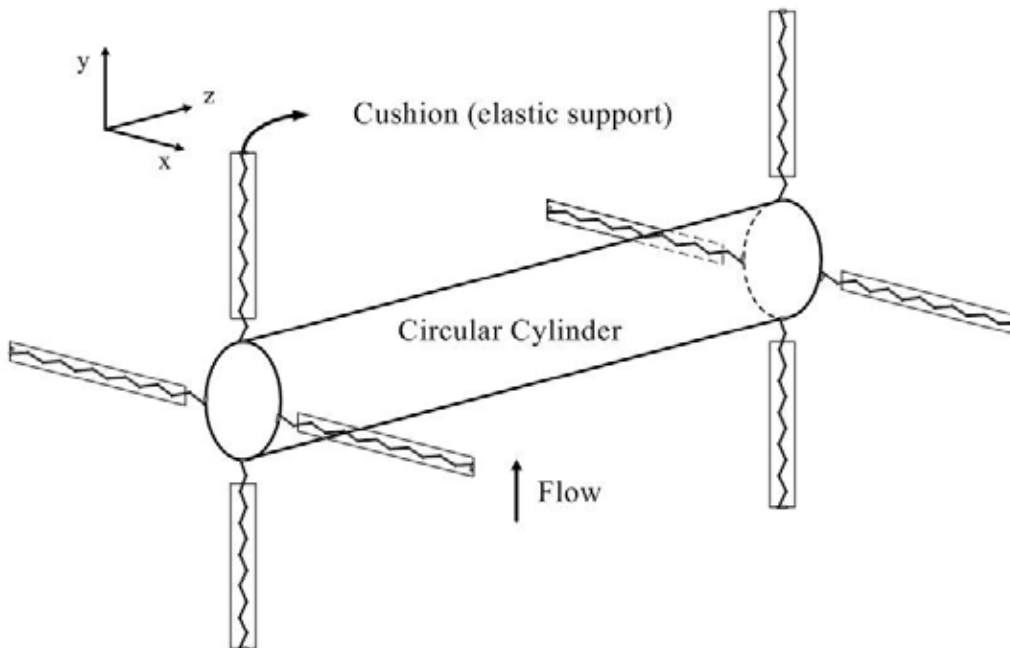


Figure 3 Elastic circular cylinder.

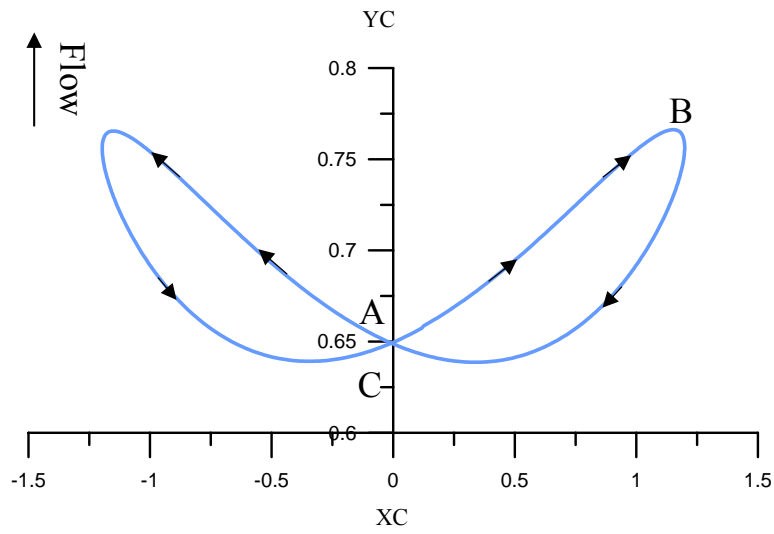


Figure 4 The periodic path of the center of the elastic cylinder.
(the Reynolds number $Re=100$, the density ratio $\rho_c = 2$, and the damping ratio $\zeta = 0$).

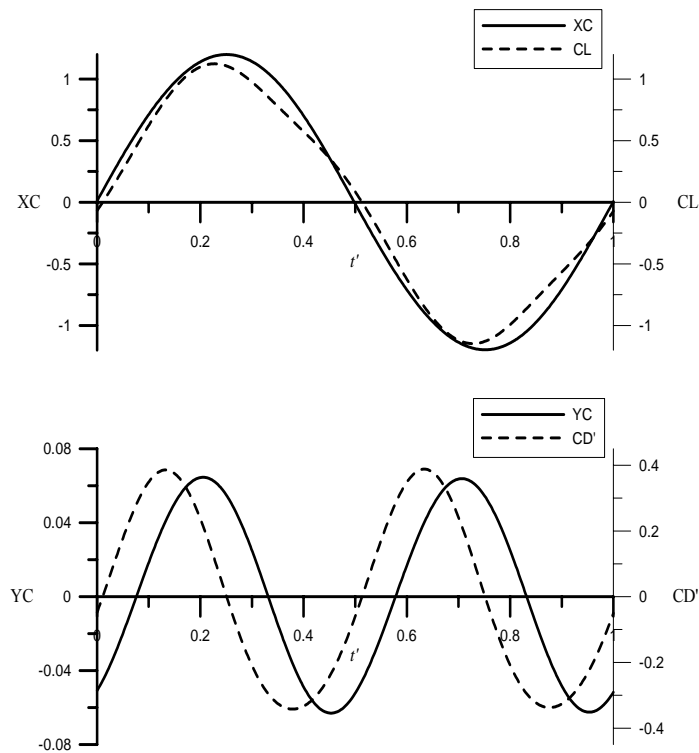


Figure 5 The periodic vibration of the forces and cylinder displacements.

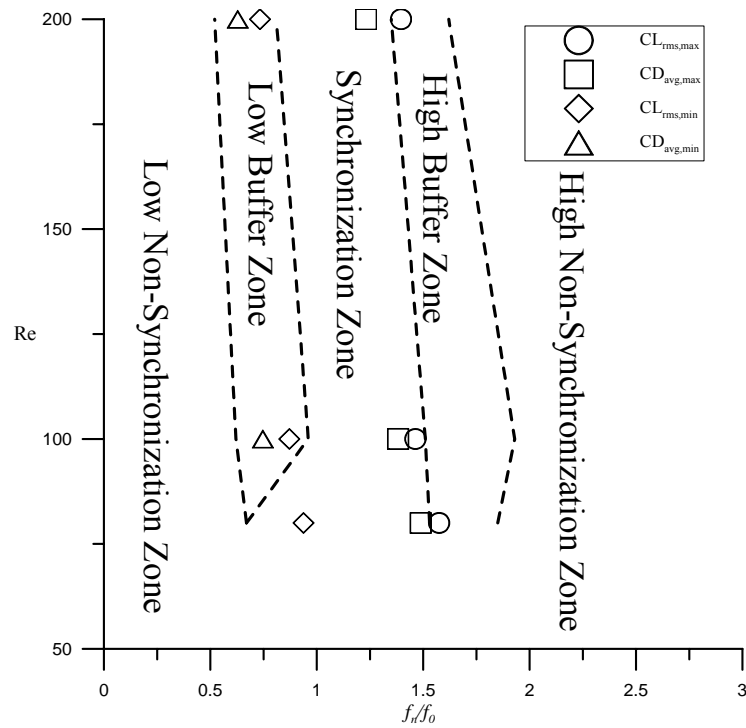


Figure 6 The vibration zones at different Reynolds number. f_0 is the vortex shedding frequency for fixed-cylinder case, and f_n is the natural frequency of the elastic cylinder.

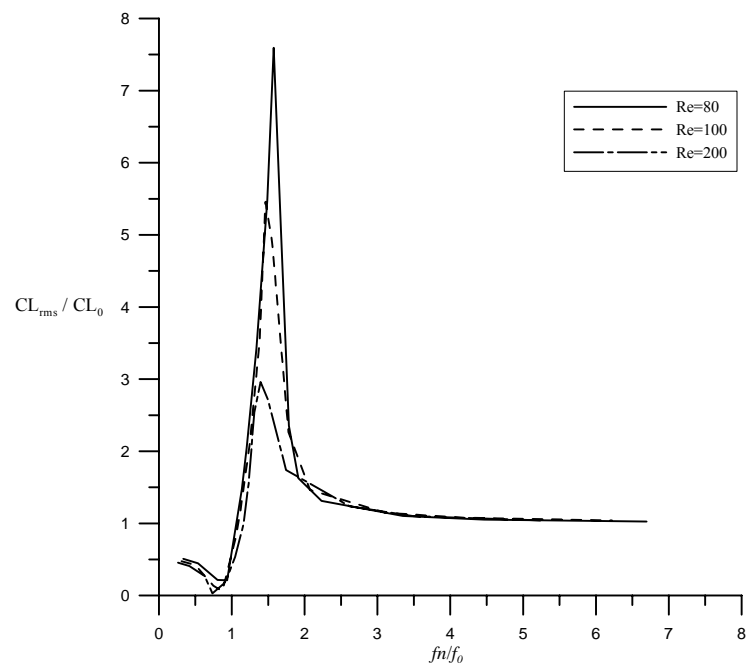


Figure 7 The curves of CL_{rms} versus f_n at different Reynolds number.

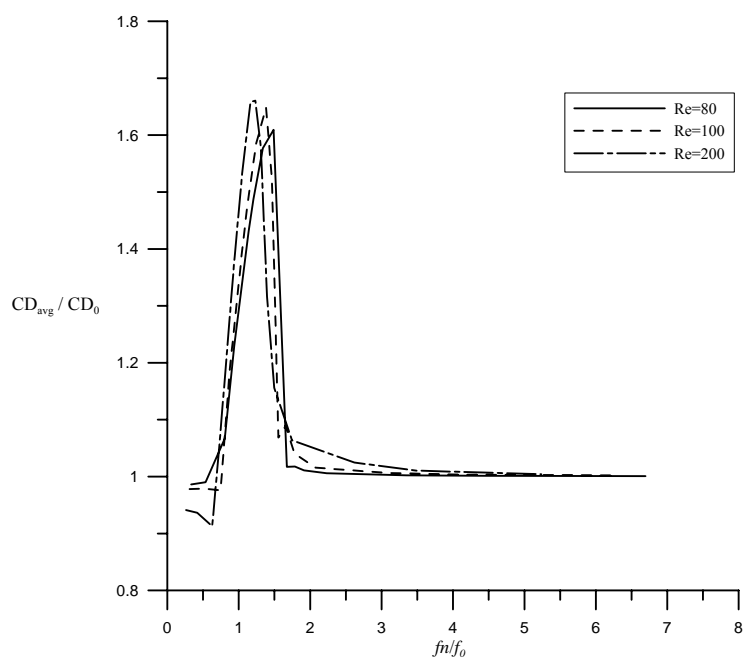


Figure 8 The curves of CD_{avg} versus f_n at different Reynolds number.